Earthline Journal of Chemical Sciences
E-ISSN: 2581-9003; CODEN: EJCSB4
Volume 12, Number 3, 2025, Pages 257-273
https://doi.org/10.34198/ejcs.12325.257273

Some isomers and tautomers of thiobarbital – A DFT treatment

Lemi Türker

Department of Chemistry, Middle East Technical University, Üniversiteler, Eskişehir Yolu No: 1, 06800 Çankaya/Ankara, Turkey
e-mail: lturker@gmail.com; lturker@metu.edu.tr

Abstract

Thiobarbital is characterized with its sedative and hypnotic properties; however it exhibits an antithyroid effect. Moreover it has a narrow range of therapeutic and toxic dose. In the present study, firstly thiobarbital and one of its structural isomer, constructed by mutual sulphur/oxygen replacements have been investigated thoroughly within the restrictions of density functional theory at the level of B3LYP/6-311++G(d,p). Secondly, its 1,3-proton tautomers have been considered at the same level of calculation. The collected data revealed that all the structures considered have exothermic heat of formation and favorable Gibbs free energy of formation values. They are thermally favored and electronically stable at the standard states. Various structural and quantum chemical data have been collected and discussed, including IR and UV-VIS spectra.

1. Introduction

Thiobarbital, also known as 5,5-diethyl-2-thiobarbituric acid, (5,5-diethyl-2-sulfanylidene-1,3-diazinane-4,6-dione) is a barbiturate derivative that has been used in medical settings for its sedative and hypnotic properties [1,2]. Thiobarbital acts on the central nervous system (CNS) by enhancing the inhibitory effects of gamma-aminobutyric acid (GABA), which is a neurotransmitter. This action results in sedative, hypnotic, and anticonvulsant effects. However, barbiturates like thiobarbital have a narrow therapeutic index, meaning the difference between an effective dose and a toxic dose is relatively small, which can lead to adverse effects and dependency.

Thiobarbital has an antithyroid effect [3-10]. Turner studied the effect on the thyroid gland of the chick [3]. Thiobarbital found some applications as intravenous anaesthestetics [11-13]. Ding investigated the comparative drug exsorption in the perfused rat intestine [14]. The content of retinal malondialdehyde (MDA) in rabbits of experimental acute ocular hypertension was determined by thiobarbital fluorescence to demonstrate the presence of retinal damage due to free radicals, and to observe the therapeutic effect of vitamin E, which is a free radical scavenger. The results indicated that free radicals participated in the retinal damage in acute ocular hypertension, and vitamin E was therapeutically effective for treatment [15].

Tautomeric forms of 2-thiobarbituric acid as studied in the solid, in polar solutions, and on gold nanoparticles were studied by Méndez et al., [16]. Supramolecular assemblies of melamine-2-thiobarbiturate were the interest of Moskalenko, et al., [17]. Kinetics of electrophilic alkylations of barbiturate and thiobarbiturate anions was investigated by Schade et al., [18]. Crystal structure, spectroscopic studies and theoretical studies of thiobarbituric acid derivatives were reported by Sharma, et al., [19].

In the present study, thiobarbital and one of its structural isomers and then some proton tautomers of thiobarbital have been investigated within the realm of density functional theory (DFT).

Received: May 18, 2025; Accepted: June 16, 2025; Published: June 19, 2025

Keywords and phrases: thiobarbital, barbital, tautomers, spectra, density functional.

2. Method of Calculations

In the present study, all the initial optimizations of the structures leading to energy minima have been achieved first by using MM2 method which is then followed by semi empirical PM3 self consistent fields molecular orbital method [20-22]. Afterwards, the structure optimizations have been achieved within the framework of Hartree-Fock and finally by using density functional theory (DFT) at the levels of B3LYP/6-311++G(d,p) [23-24]. Note that the exchange term of B3LYP consists of hybrid Hartree-Fock and local spin density (LSD) exchange functions with Becke's gradient correlation to LSD exchange [25]. The correlation term of B3LYP consists of the Vosko, Wilk, Nusair (VWN3) local correlation functional [26] and Lee, Yang, Parr (LYP) correlation correction functional [27]. In the present study, the normal mode analysis for each structure yielded no imaginary frequencies for the 3*N*–6 vibrational degrees of freedom, where *N* is the number of atoms in the system. This search has indicated that the structure of each molecule considered corresponds to at least a local minimum on the potential energy surface. Furthermore, all the bond lengths have been thoroughly searched in order to find out whether any bond cleavage occurred or not during the geometry optimization process. All these computations were performed by using SPARTAN 06 program [28].

3. Results and Discussion

Figure 1 stands for the optimized structures of the thiobarbital isomers considered. The figure also displays the direction of the dipole moment vectors.

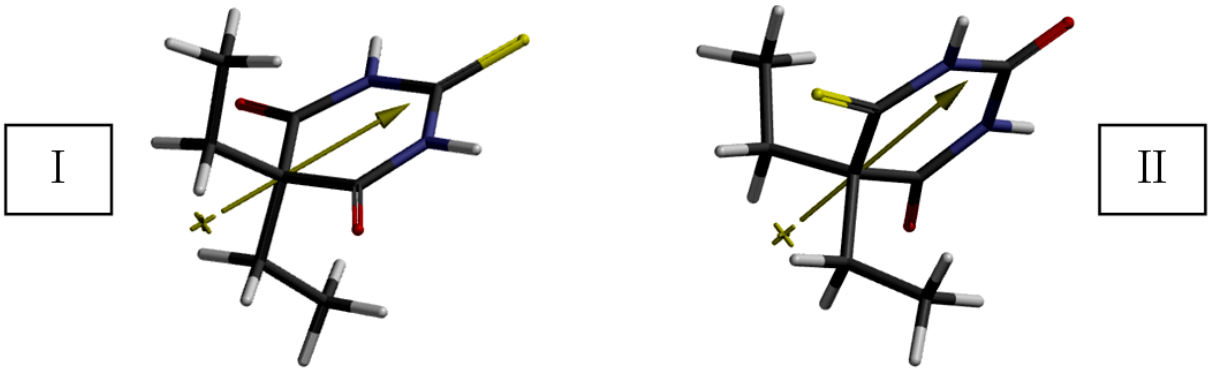

Figure 1. Optimized structures of the isomers considered.

Table 1 shows some of the standard thermo chemical formation data of the species considered. The data reveal that the standard heat of formation (H°) values of all the species are exothermic, and they are favored according to their G° (Gibbs free energy of formation) values. The algebraic order of H° and G° values for isomeric tautomers are the same as I<II.

Table 1. Some thermo chemical properties of the isomers considered.

Isomers	H°	S° (J/mol°)	G°
I	-2547420.637	437.94	-2547551.209
II	-2547417.271	436.26	-2547547.342

Energies in kJ/mol.

Table 2 shows some energies of the species considered where E, ZPE and E_C stand for the total electronic energy, zero point vibrational energy and the corrected total electronic energy, respectively. According to the

data, they are all electronically stable structures. The stability order for isomeric species is I>II. Note that the sulphur atom in structure-II causes more steric hindrance as compared to structure-I. Also note that in thiobarbital (I), the thiocarbonyl moiety is flanked by two amino groups whereas in isomer-II the thiocarbonyl moiety has only one amino neighbor. Thus the electronic effects in two cases are quite different.

Table 2. Some energies the isomers considered.

Isomers	E	ZPE	E_C
I	-2547957.70	527.87	-2547429.83
II	-2547954.46	528.13	-2547426.33

Energies in kJ/mol.

Some calculated properties of the thiobarbital isomers considered are shown in Table 3. Note that isomer-I has a greater area but smaller volume compared to isomer-II. It is worth mentioning that the polar surface area (PSA) is defined as the amount of molecular surface area arising from polar atoms (N,O) together with their attached hydrogen atoms. Although these compounds are isomeric, their PSA values differ from each other, meaning that the same kind of atoms might be influenced by electronic factors differently at different positions.

Table 3. Some properties of the thiobarbital isomers considered.

Isomer	Area (Å²)	Volume (Å³)	PSA (Å²)	Ovality	Log P
I	214.04	189.76	51.245	1.34	1.29
II	213.07	189.79	51.120	1.33	1.29

As for the log P values, all the species considered have log P values which are positive. Note that a negative value for log P means the compound has a higher affinity for the aqueous phase (it is more hydrophilic); when log P = 0 the compound is equally partitioned between the lipid and aqueous phases; whereas a positive value for log P denotes a higher concentration in the lipid phase (i.e., the compound is more lipophilic).

Table 4 shows some other properties of the thiobarbital isomers considered. Since the total dipole moment is the vectorial some of bond dipoles, the isomers have very different dipole moment values.

Table 4. Some other properties of the thiobarbital isomers considered.

Isomer	Dipole moment	Polarizability	E_{aq}	E_{solv}
I	1.44	55.74	-2547999.53	-48.767
II	0.97	55.78	-2547990.45	-44.706

Dipole moments in debye. Polarizabilities in 10^{-30} m^3 units. Energies in kJ/mol. Solvation energy by SM5.4/A model. E_{solv}: PM3//B3LYP/6-311++G(d,p).

Aqueous and solvation energy values (E_{aq} and E_{solv}, respectively) for the species considered are shown also in Table 4. The algebraic order of aqueous and solvation energy values for isomeric thiobarbital species are the same that is I<II.

The calculated IR spectrums of the isomers considered are shown in Figure 2. In the case of isomer-I, the N-H stretchings of thioamide/amide happen at 3577 cm^{-1} (symmetrical) and 3571 cm^{-1} (unsymmetrical). All the C-H stretchings of the ethyl groups accumulated in between 3112 cm^{-1} and 3000 cm^{-1}. The peaks at 1788 cm^{-1}

and 1757 cm^{-1} belong to C=O stretchings. The sharp peat at 1544 cm^{-1} is the bending vibrations of thioimide hydrogens coupled with C=S stretch.

As for the spectrum of isomer-II, the N-H stretchings of imide happen at 3577 cm^{-1} (between two carbonyls) and 3562 cm^{-1} (near C=S moiety). The weak peaks in between 3114 cm^{-1} and 3000 cm^{-1} belong to C-H stretchings. The carbonyl stretchings occur at 1806 cm^{-1} and 1775 cm^{-1}. The weak peak at 1405 cm^{-1} is C=S stretching overlapped with various N-H and C-H bending vibrations.

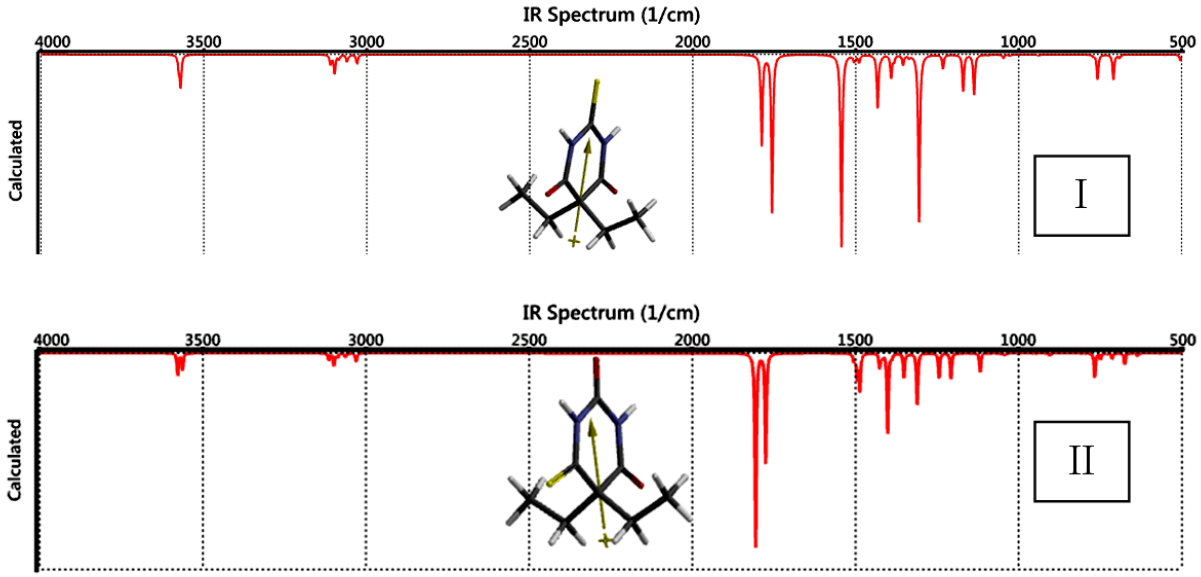

Figure 2. The calculated IR spectrums of the isomers considered.

Figure 3 displays the electrostatic potential (ESP) charges on atoms of the isomers considered. Note that the ESP charges are obtained by the program based on a numerical method that generates charges that reproduce the electrostatic potential field from the entire wavefunction [28].

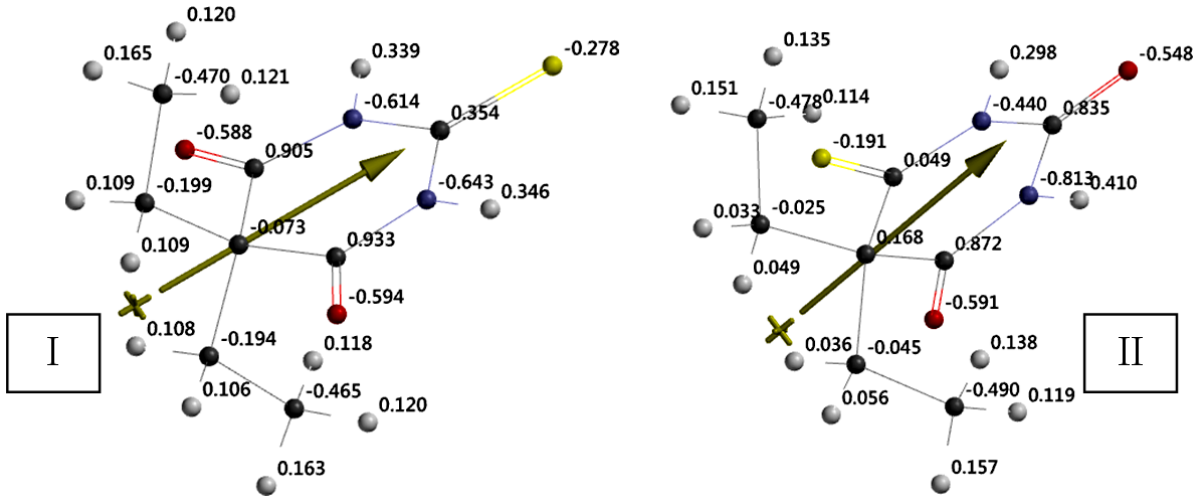

Figure 3. The ESP charges on atoms of the isomers considered.

Electrostatic potential maps of the isomers considered are shown in Figure 4, where negative potential regions reside on red/reddish and positive ones on blue/bluish parts of the maps.

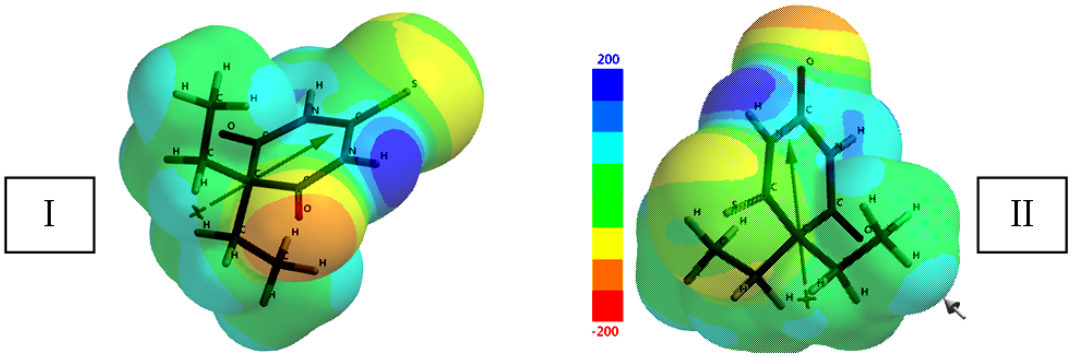

Figure 4. ESP maps of the isomeric thiobarbital species considered.

Figure 5 shows the exposed area of atoms in the isomers considered [29]. Note that the exposed surface areas of sulphur atom in isomer-II is smaller compared to the respective value in isomer-I. A similar decrease occurs for the oxygen atom of carbonyl nearby the ethyl substituent.

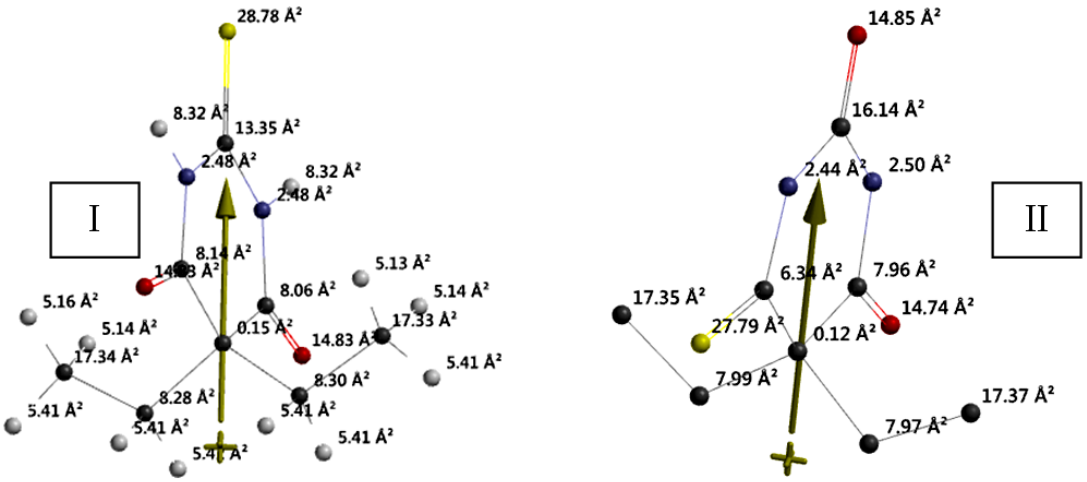

Figure 5. Exposed area of atoms in the isomers considered.

Figure 6 displays the calculated bond lengths of the isomers (Hydrogens excluded).

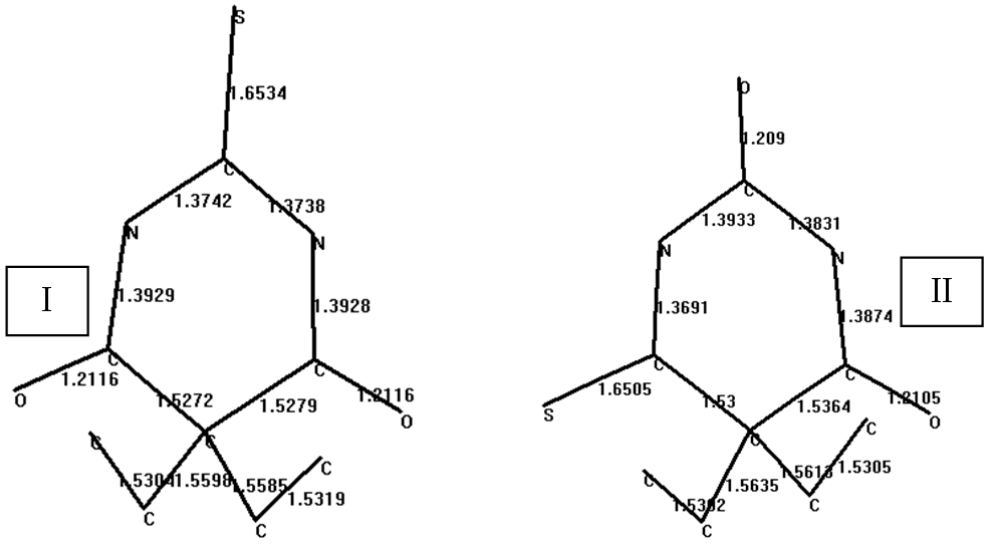

Figure 6. The calculated bond lengths of the isomers (Hydrogens excluded).

As seen in the figure bond lengths of the ring are different in two isomers. It arises from the relatively bulkier sulphur atom which causes different steric and electronic effects at different positions. The same types of bond lengths vary from one structure to other. Although the variations are small in most of the cases, it indicates that structural and electronic effects vary from structure to structure. For instance some of the internal bond angles of the ring in isomer-I are C=O; 117.61°, 117.59° and C=S: 114.65° whereas the respective ones in isomer-II are C=O; 114.39 °, 117.77 ° and C=S: 117.16 °.

Figure 7 shows the local ionization maps of the isomeric thiobarbital species considered where conventionally red/reddish regions (if any exists) on the density surface indicate areas from which electron removal is relatively easy, meaning that they are subject to electrophilic attack. It is worth remembering that the local ionization potential map is a graph of the value of the local ionization potential on an isodensity surface corresponding to a van der Waals surface.

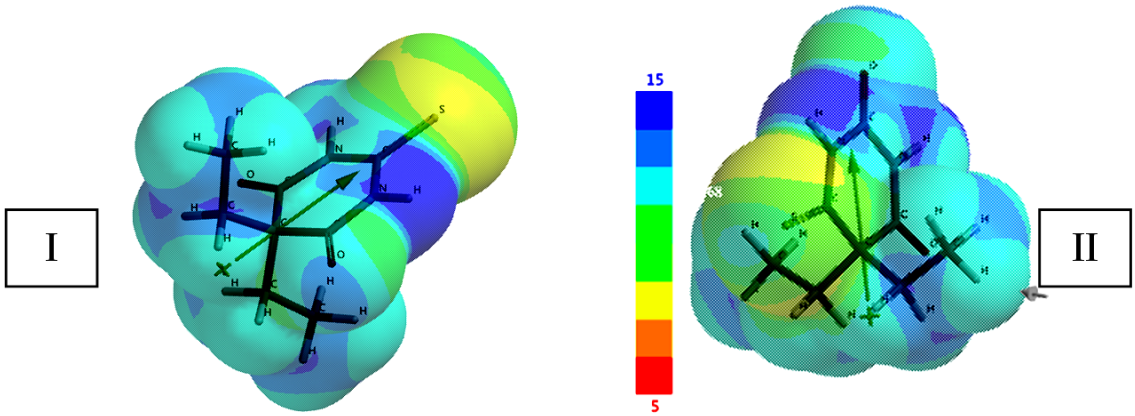

Figure 7. The local ionization maps of the isomeric thiobarbital species considered.

Figure 8 stands for the LUMO maps of the isomeric thiobarbital species considered. Note that a LUMO map displays the absolute value of the LUMO on the electron density surface. The blue color (if any exists) stands for the maximum value of the LUMO and the red colored region, associates with the minimum value. Note that the LUMO and NEXTLUMO are the major orbitals directing the molecule towards the attack of nucleophiles [30,31]. Positions where the greatest LUMO coefficient exists is the most vulnerable site in nucleophilic reactions.

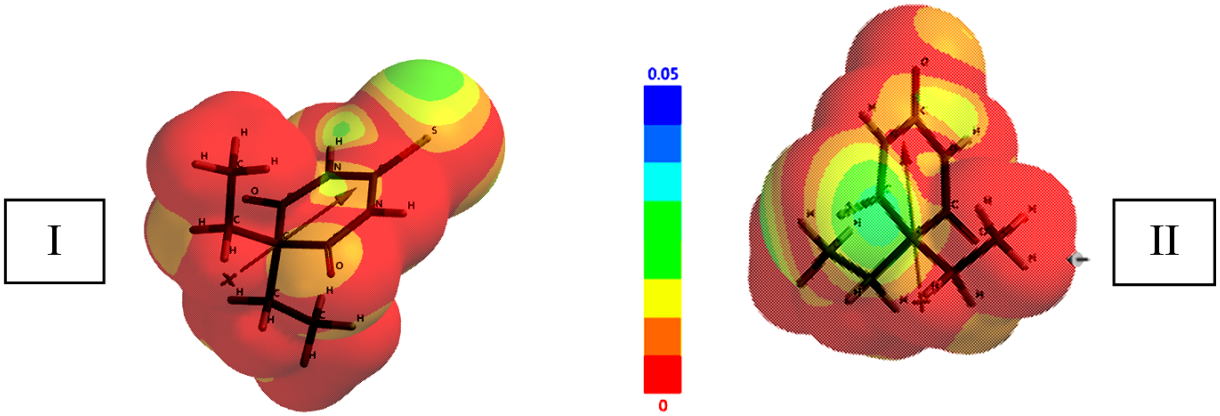

Figure 8. The LUMO maps of the isomeric thiobarbital species considered.

Figure 9 shows the bond density maps of the isomeric thiobarbital species considered, (focused on the ring atoms).

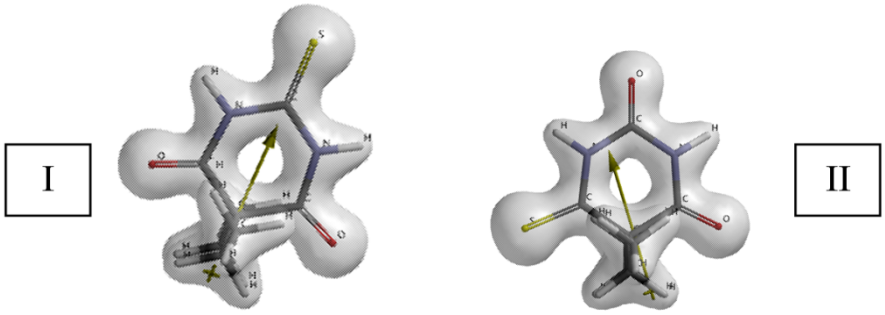

Figure 9. The bond density maps of the isomeric thiobarbital species considered.

Figure 10 shows some of the orbital energy levels of the isomeric thiobarbital species considered. It is to be noted that density of the inner lying molecular orbitals are indicative of thermal stability.

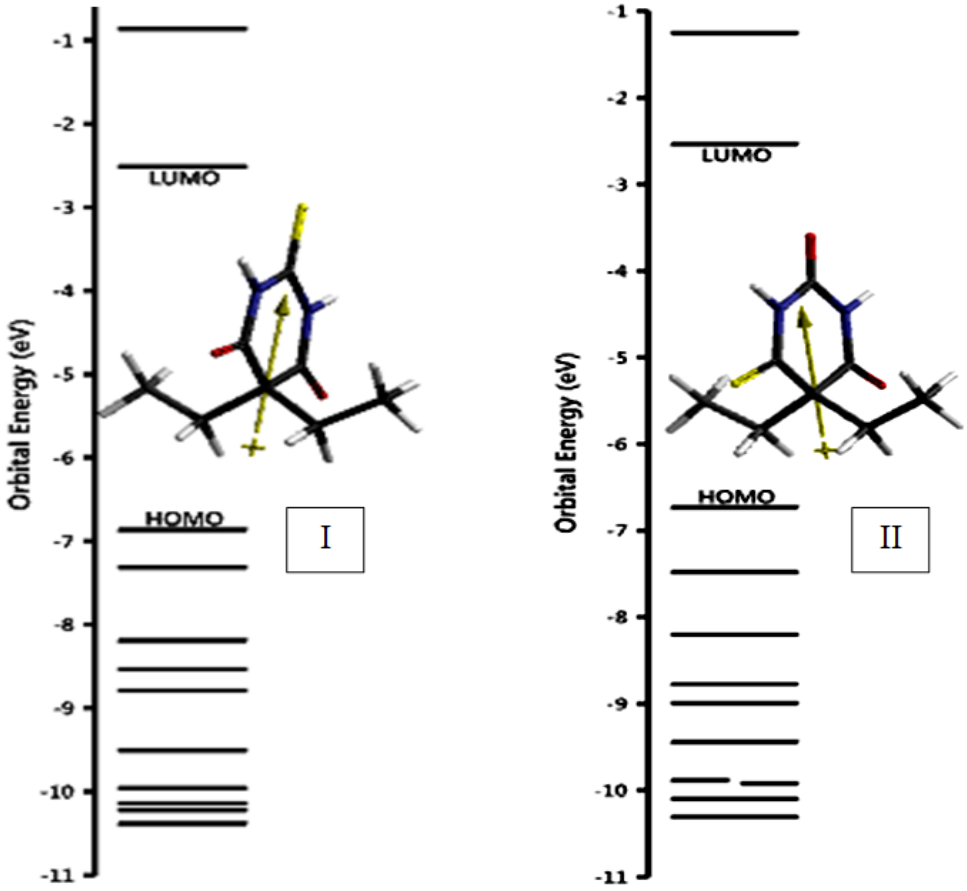

Figure 10. Some of the orbital energy levels of the isomeric thiobarbital species considered.

Table 5 lists the HOMO, LUMO energies and the interfrontier molecular orbital energy gap Δε [30,31] values ($\Delta\varepsilon = \varepsilon_{LUMO}-\varepsilon_{HOMO}$) of the isomers considered. The algebraic orders of the HOMO and LUMO energies are I<II and II<I, respectively. Consequently, the order of Δε values becomes II<I. In these isomers interchange of positions of sulphur and oxygen atoms raises the HOMO but lowers the LUMO energy levels of II with respect to isomer-I. All the geometrical and electronic factors should be responsible for that. The mesomeric effect(s) of amide/imide nitrogens operative on the carbonyl and thiocarbonyl moieties are to be considered.

Table 5. The HOMO, LUMO energies and Δε values of the isomers considered.

Isomers	HOMO	LUMO	Δε
I	-662.54	-241.96	420.58
II	-649.54	-244.54	405.00

Energies in kJ/mol.

Figure 11 shows the HOMO and LUMO patterns of the isomeric species considered. As seen in the figure, they have π-symmetry in great extent. The sulphur atom has a greater contribution to the HOMO and LUMO in both of the isomers compared to the contributions coming from the oxygen atoms.

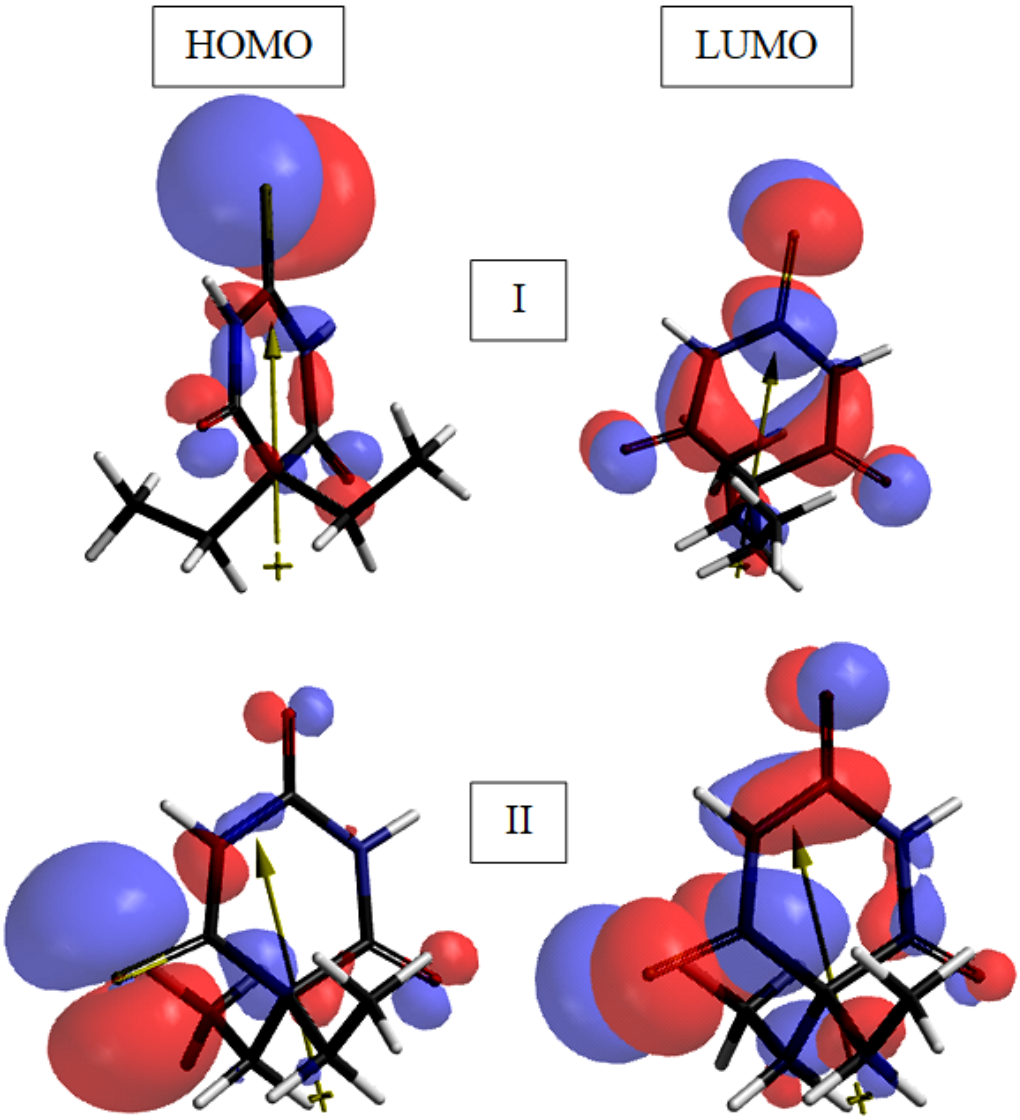

Figure 11. The HOMO and LUMO patterns of the isomeric species considered.

Figure 12 displays the calculated UV-VIS (time dependent DFT) spectra of the isomers considered. As seen in the figure, both of the isomers mainly absorb in the UV region. The rather weak absorbance of isomer-I in the 350-420 nm shifts to visible region (350-500 nm) in isomer-II which is expected as Δε values of the isomers are considered (see Table 5). Also its intensity increases considerably.

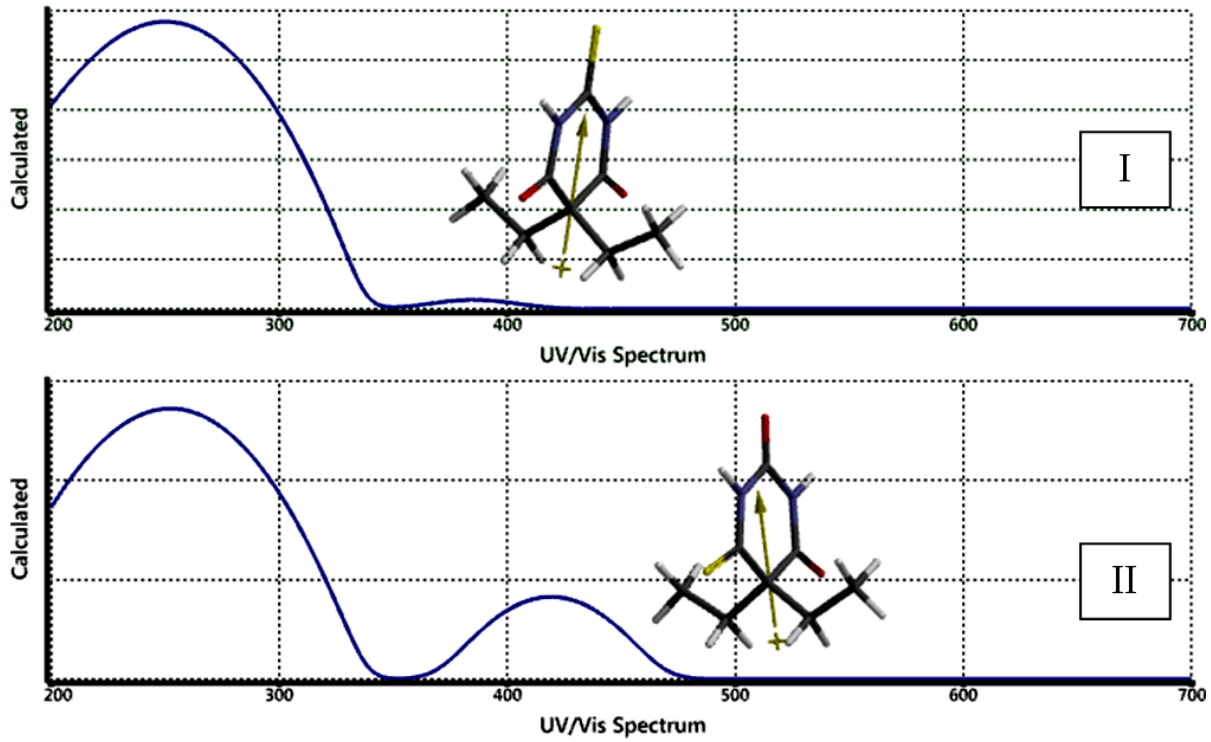

Figure 12. The calculated UV-VIS spectra of the isomers considered.

Tautomers

Figure 13 shows the optimized structures as well as the direction of the dipole moment vectors of the tautomers presently considered. Thiobarbital (I) which is more stable than isomer-II possesses two N-H moieties linked to the carbonyl / thiocarbonl groups which may undergo 1,3-type proton tautomerism.

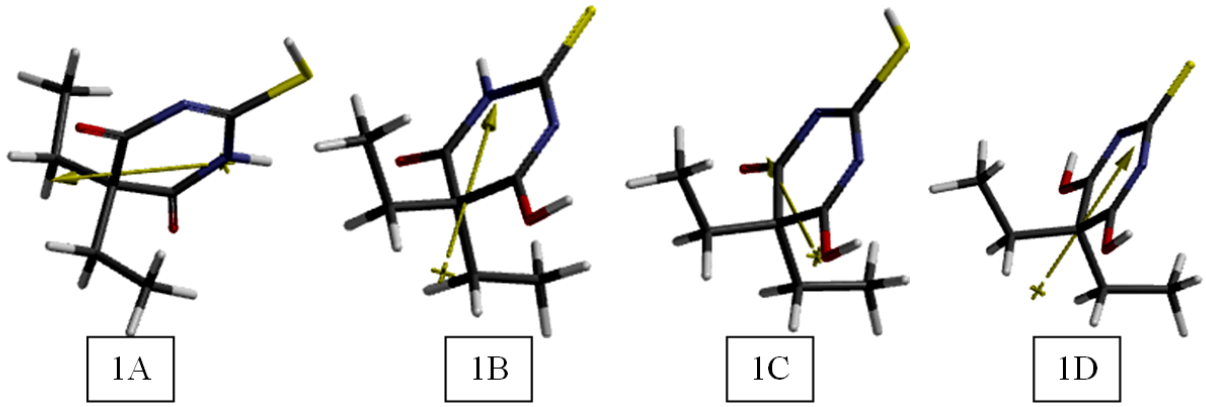

Figure 13. Optimized structures of the tautomers considered.

Table 6 shows some thermo chemical properties of the tautomers considered. It also includes the respective values for isomer-I. They have all exothermic heat of formation values and favorable Gº values. The orders of Hº and Gº are the same as I<1B<1A<1C<1D. The electronic stabilities of the species considered follow the same order. It seems that in these structures the proton on sulphur leads to a tautomer which is less exothermic and less stable than the one on nitrogen. In general the tautomers having double proton shift (1C,1D) are less exothermic and less stable than the singly occurred ones (1A,1B).

Table 6. Some thermo chemical properties of the tautomers considered.

Tautomers	Hº	Sº (J/molº)	Gº
I	-2547420.637	437.94	-2547551.209
1A	-2547343.512	444.82	-2547476.135
1B	-2547355.324	438.24	-2547485.989
1C	-2547302.391	442.84	-2547434.426
1D	-2547279.244	438.71	-2547410.048

Energies in kJ/mol.

Table 7 lists some energies of isomer-I and its tautomers considered. The electronic stabilities of the species considered follow the order of I<1B<1A<1C<1D. Thus the stability decreases as the embedded imide/ thioimide moieties are converted to the respective imidol type moieties.

Table 7. Some energies the tautomers considered.

Tautomers	E	ZPE	E_C
I	-2547957.70	527.87	-2547429.83
1A	-2547871.00	517.11	-2547353.89
1B	-2547891.45	526.82	-2547364.63
1C	-2547829.77	517.37	-2547312.4
1D	-2547814.66	525.93	-2547288.73

Energies in kJ/mol.

Figure 14 displays the ESP charges on atoms of the tautomers considered. Figure 15 stands for the ESP maps of the tautomers considered. Note that negative potential regions reside on red/reddish and positive ones on blue/bluish parts of the maps.

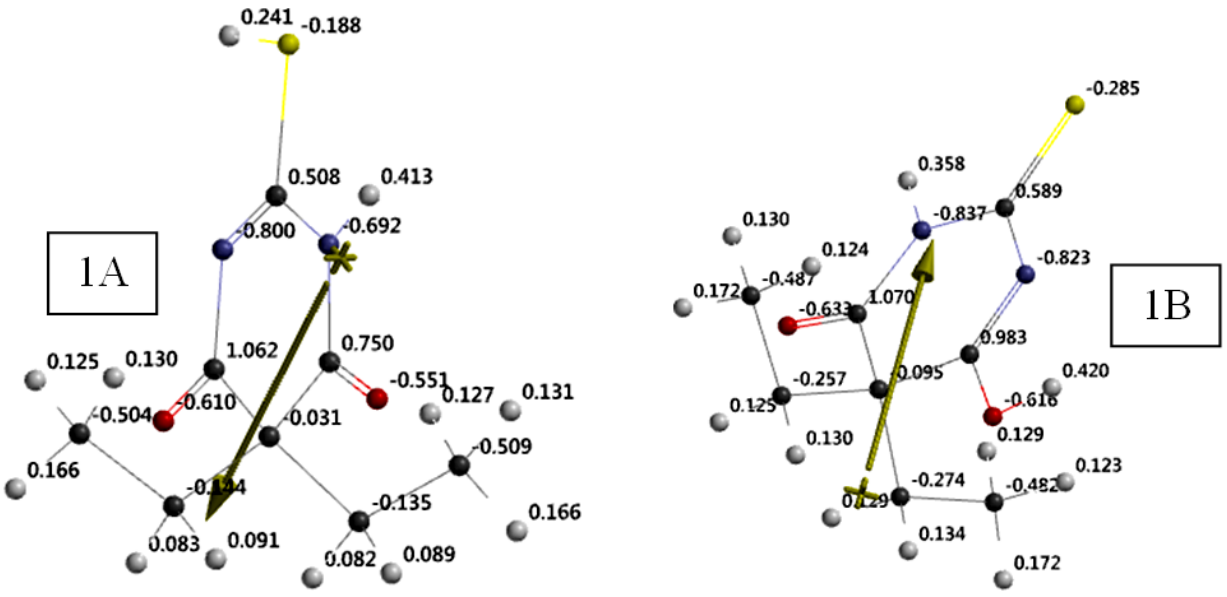

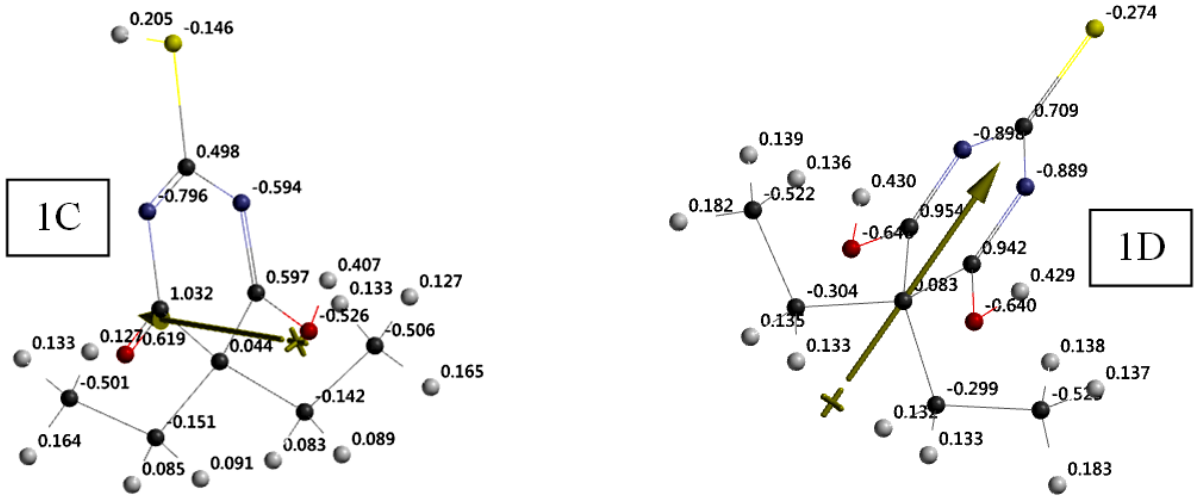

Figure 14. The ESP charges on atoms of the tautomers considered.

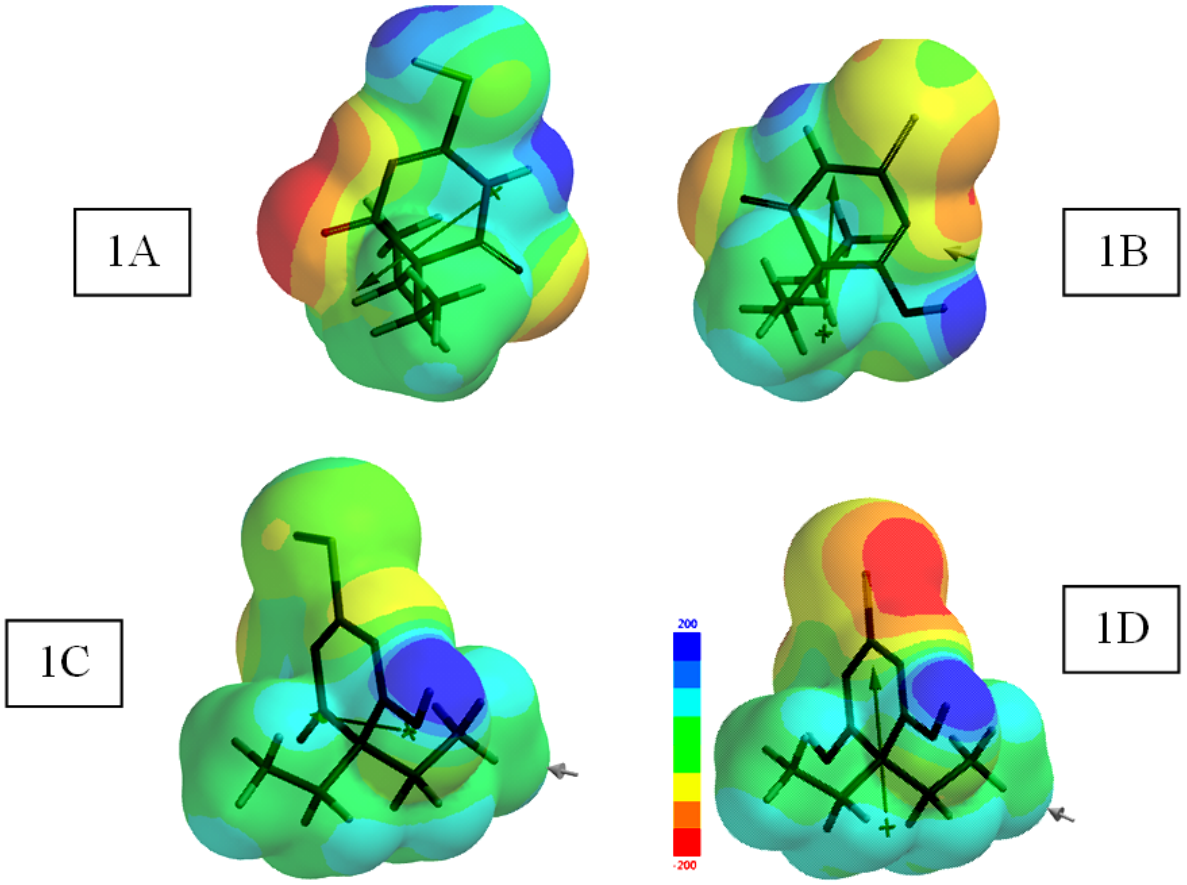

Figure 15. The ESP maps of the tautomers considered.

The local ionization maps of the tautomers considered are shown in Figure 16. Also note that red/reddish regions (if any exists) on the density surface indicate areas from which electron removal is relatively easy, meaning that they are subject to electrophilic attack.

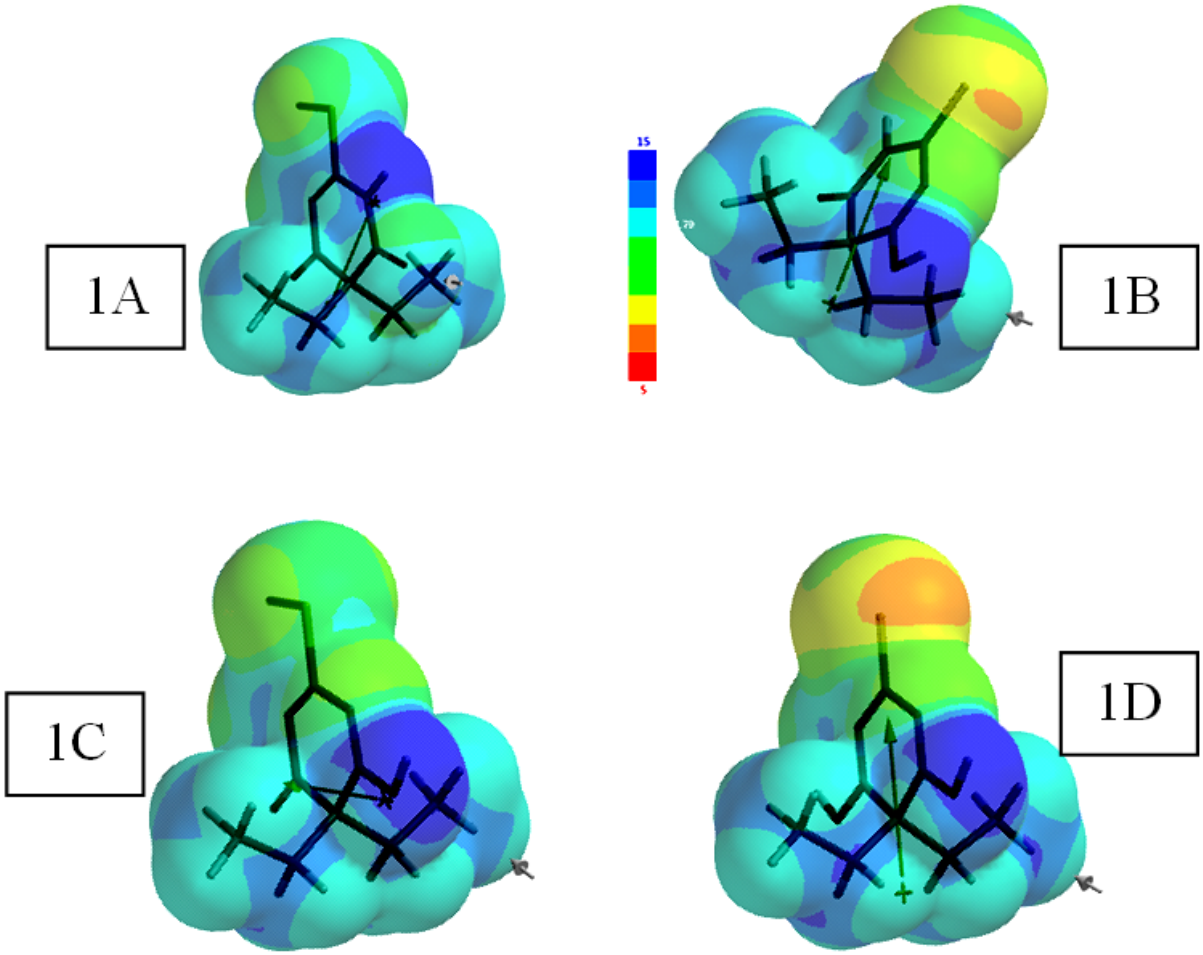

Figure 16. The local ionization maps of the tautomers considered.

Figure 17 shows the LUMO maps of the tautomers presently considered. The blue color (if any exists) stands for the maximum value of the LUMO and the red colored region, associates with the minimum value. The LUMO and NEXTLUMO are the major orbitals directing the molecule towards of the attack of nucleophiles [31]. Note that position possessing the greatest LUMO coefficient is the most vulnerable site in nucleophilic reactions.

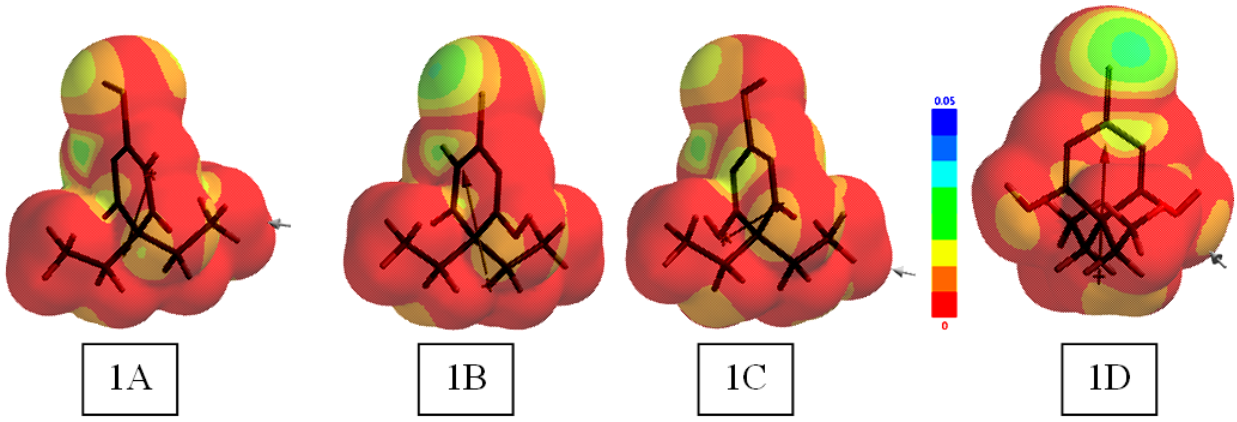

Figure 17. The LUMO maps of the tautomers considered.

Figure 18 shows the calculated IR spectrums of the tautomers considered. In spectrum of 1A, N-H stretching occurs at 3573 cm^{-1}, followed by various C-H stretchings around 3000 cm^{-1}. The S-H stretching occurs at 2752 cm^{-1} whereas C=O stretchings take place at 1789 cm^{-1} and 1758 cm^{-1}. The sharp peak at 1612 cm^{-1} stands for N-H bending.

In spectrum of 1B, 3722 cm^{-1} is the O-H stretching of the tautomer followed by N-H stretching occurring at 3566 cm^{-1}. The moderately sharp peak at 1768 cm^{-1} is the carbonyl stretching followed by the ring vibrations at 1651 cm^{-1} (sharp) coupled with O-H bendings. The C=S stretching happens at 1140 cm^{-1} overlapped with various bending motions.

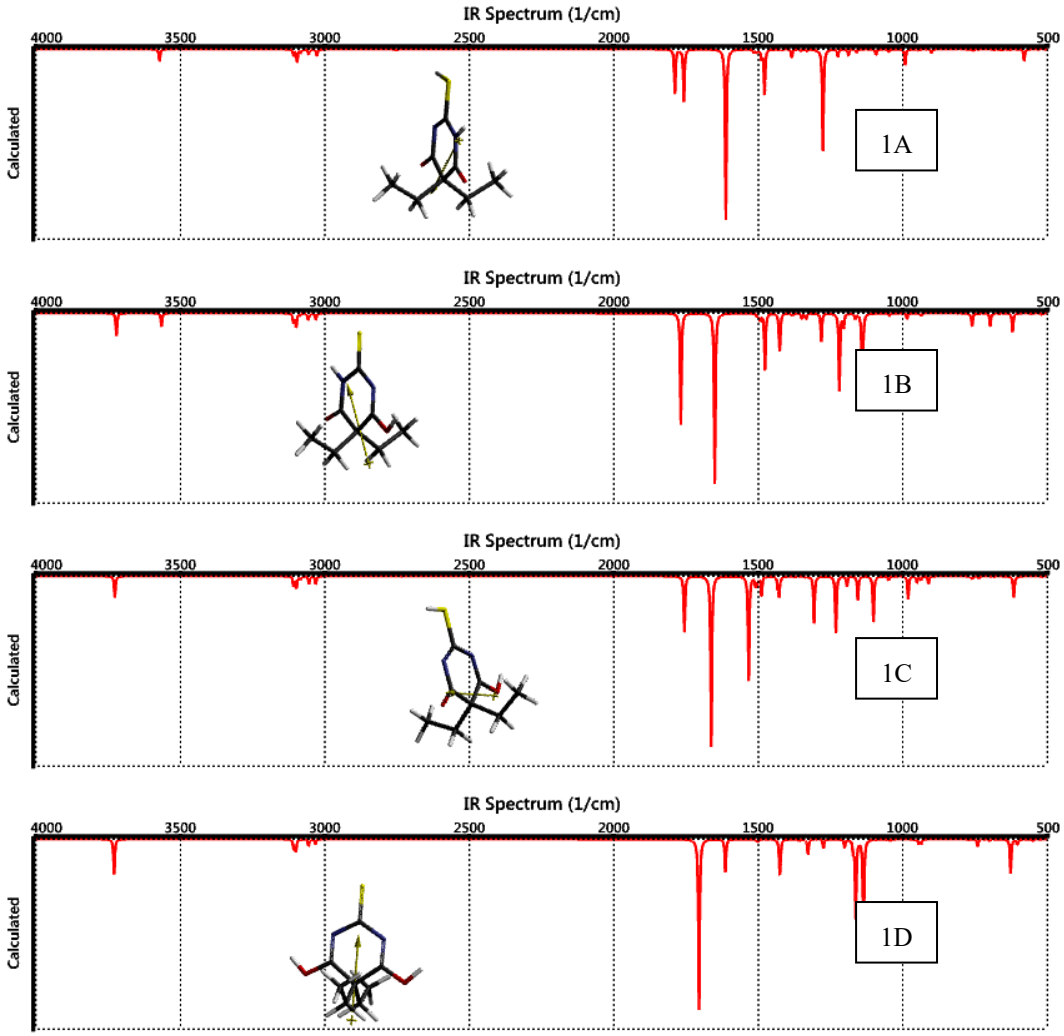

Figure 18. The calculated IR spectrums of the tautomers considered.

In spectrum of 1C, O-H stretching is at 3727 cm^{-1} whereas S-H stretching is observed at 2731 cm^{-1}(very weak). The peak at 1756 cm^{-1} stands for C=O stretch. 1663 cm^{-1} and 1533 cm^{-1} are ring vibrations accompanied by various bendings.

The O-H stretching of 1D appears at 3730 cm^{-1} and various C-H vibrations occur at 3108 -3033 cm^{-1}. The sharp peak at 1705 cm^{-1} stands for the ring vibrations comprising the C=S stretch. The weak peak at 1614 cm^{-1} is the ring vibrations accompanied by O-H bendings.

Table 8 shows some properties of the tautomers considered. The order of dipole moments and the polarizabilities are the same as 1D>1B>1C>1A.

Table 8. Some properties of the tautomers considered.

Tautomers	Dipole moment	Polarizability	E_{aq}
1A	2.82	55.60	-2547913.93
1B	4.09	55.86	-2547953.01
1C	3.89	55.66	-2547883.57
1D	5.76	55.96	-2547901.83

Energies in kJ/mol. Dipole moments in debye. Polarizabilities in 10^{-30} m^3 units.

Table 9 tabulates the HOMO, LUMO (frontier molecular orbitals) energies and Δε values of the parent isomer-I and its tautomers considered. Order of the HOMO energies is 1A<1C<I<1B<1D whereas the LUMO energies follow the order of 1B<1D<I<1C<1A. Consequently, the interfrontier molecular orbital energy gap values (Δε) construct the order of 1D<1B<I<1C<1A. Hence, the character of 1,3 proton tautomerism (single or double) occurred in isomer-I (thiobarbital) is/are highly influential on the frontier molecular orbitals and their energies of the tautomers derived from the parent structure which are the consequence of skeletal and electronic variations accompanied.

Table 9. The HOMO, LUMO energies and Δε values of the tautomers considered.

Tautomers	HOMO	LUMO	Δε
I	-662.54	-241.96	420.58
1A	-708.20	-220.75	487.45
1B	-616.09	-256.26	359.83
1C	-691.30	-241.08	450.22
1D	-563.91	-250.47	313.44

Energies in kJ/mol.

Figure 19 shows the calculated (time dependent DFT) UV-VIS spectra of the tautomers considered. As seen in the figure, they all mainly absorb in the UV region. However, 1B,1C and 1D have some absorbance in the visible part. Among the tautomers, 1D is characterized with the smallest Δε value (even smaller than isomer-I has) possesses the longest λ_{max} value in the visible region. Tautomer-1A has a huge shoulder probably arising from conjugation involving the embedded imide and amide moieties as well as the thione moiety present in the parent compound thiobarbital. Since the calculated spectra involve not only the HOMO-LUMO excitations, some of the spectra possess shoulders or overlapped peaks. The calculated intensities of the peaks related to magnitudes of the transition moments varying from tautomer to tautomer.

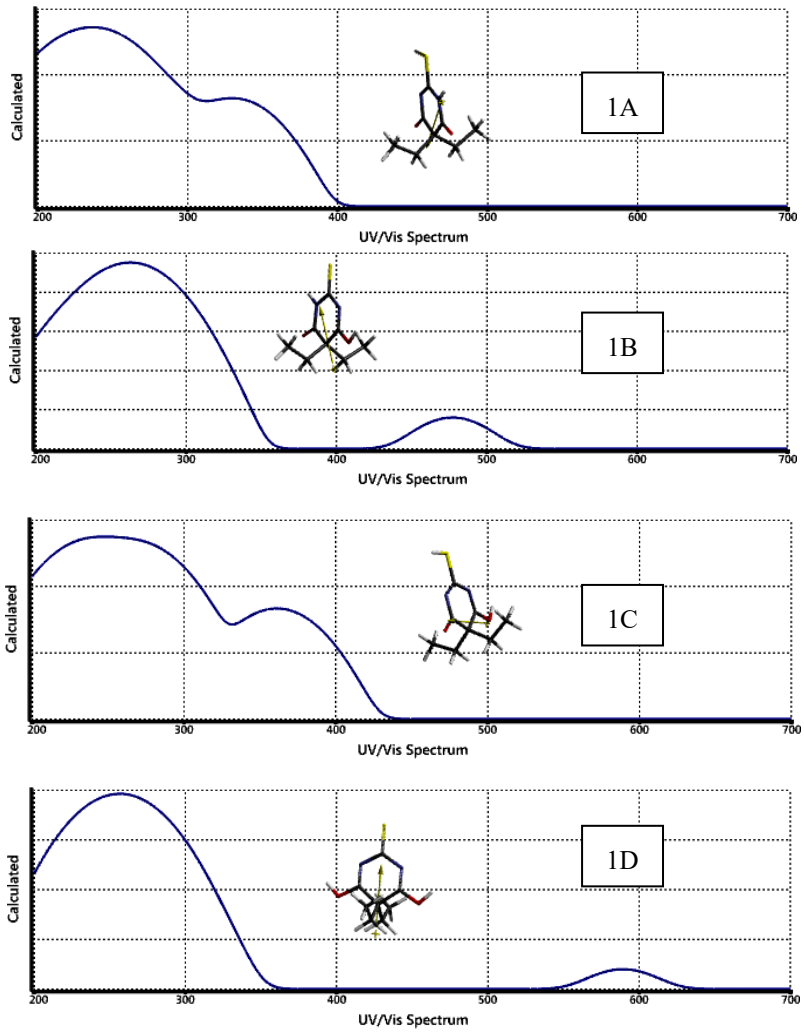

Figure 19. The calculated UV-VIS spectra of the tautomers considered.

4. Conclusion

In the present computational study, thiobarbital and one of its structural isomers and some of its 1,3-proton tautomers, are considered within the restrictions of density functional theory. In the vacuum conditions, all of them are characterized with exothermic heat of formations and favorable Gibbs free energy of formation values and they are all electronically stable. The results collected indicated that the character of 1,3-proton tautomerism (single or double) occurred in isomer-I (thiobarbital) is/are highly influential on the various properties including the frontier molecular orbitals and their energies of the tautomers derived from the parent structure, as the consequence of skeletal and electronic variations accompanied. Structural isomers of thiobarbital might be worth investigated in order to get compounds having better performance but less harmful. On the other hand, mutual interaction between the thiobarbital and its tautomers in aqueous conditions might be interesting.

References

[1] Fischer, E., & Dilthey, A. (1904). Ueber C-Dialkylbarbitursäuren und über die Ureïde der Dialkylessigsäuren. *Justus Liebigs Annalen der Chemie*, *335*(3), 334-368. https://doi.org/10.1002/jlac.19043350303

[2] Carrington, H.C. (1944). The action of phosphorus pentasulphide on barbituric acids. *Journal of the Chemical Society* (*Resumed*), 124-126. https://doi.org/10.1039/JR9440000124

[3] Turner, C.W. (1946). Comparison of the effect of feeding thiobarbital and thiouracil on the thyroid gland of the chick. *Poultry Science*, *25*(5), 517-520. https://doi.org/10.3382/ps.0250517

[4] Bartels, E.C. (1945). Use of thiobarbital in the treatment of hyperthyroidism. *JAMA*, *129*(14), 932-935. https://doi.org/10.1001/jama.1945.02860480012003

[5] Astwood, E.B. (1945). Some observations on the use of thiobarbital as an antithyroid agent in the treatment of graves' disease. *The Journal of Clinical Endocrinology & Metabolism*, *5*(8), 345-352. https://doi.org/10.1210/jcem-5-8-345

[6] Bartels, E.C. (1945). Use of thiobarbital in the treatment of hyperthyroidism. *JAMA*, *129*(14), 932-935. https://doi.org/10.1001/jama.1945.02860480012003

[7] Bush, M.T., Mazel, P., & Chambers, J. (1961). The metabolic fate of thiobarbiturates: thiobarbital in man. *The journal of Pharmacology and Experimental Therapeutics, 134(1*), 110-116. https://doi.org/10.1016/S0022-3565(25)26137-7

[8] Lahey, F.H., Bartels, E.C. (1947). The use of thiouracil, thiobarbital and propyl thiouracil in patients with hyperthyroidism. *Annals of Surgery, 125*(5), 572-581.

[9] Mansberger, A.R., Jr. (1988). One hundred years of surgical management of hyperthyroidism. *Ann. Surg., 207*(6), 724-9. https://doi.org/10.1097/00000658-198806000-00012. PMID: 3291793; PMCID: PMC1493546.

[10] McGavack, T.H. (1948). Status of antithyroid substances in thyroid disease. *The American Journal of Medicine*, *5*(1), 90-99. https://doi.org/10.1016/0002-9343(48)90014-X

[11] Németh, S., Viskupic, E., & Murgas, K., (1985). Intravenous thiobarbital anaesthesia for determination of liver glycogen phosphorylase activity in rats subjected to various forms of stress. *Endocrinologia Experimentalis*, *19*(2), 91-95. PMID: 3874768.

[12] Bloch, A., Bock, A., Dietz, O., Litzke, L.F., & Moldenhauer, R. (1986). New practicable techniques for injection anaesthesia in swine. *Monatshefte für Veterinärmedizin*, *41*(15), 534-537.

[13] Paulin, J., & Lofgren, J. (2023). Anesthesia and analgesia in laboratory rodents. In M. C. Dyson, P. Jirkof, J. Lofgren, E. A. Nunamaker, & D. Pang (Eds.), *American College of Laboratory Animal Medicine* (3rd ed., Chapter 14, pp. 287-356). New York: Academic Press. https://doi.org/10.1016/B978-0-12-822215-7.00007-X

[14] Huang, J.-D. (1990). Comparative drug exsorption in the perfused rat intestine. *Journal of Pharmacy and Pharmacology, 42*, 167-170. https://doi.org/10.1111/j.2042-7158.1990.tb05378.x

[15] Zhao, G.Q. (1993). Free radical retinal damage in rabbits of experimental acute ocular hypertension. *Chinese Journal of Ophthalmology*, *29*(5), 293-295. PMID: 8168396.

[16] Méndez, E., Cerdá, M.F., Gancheff, J.S., Torres, J., Kremer, C., Castiglioni, J., Kieninger, M., & Ventura, O.N. (2007). Tautomeric forms of 2-thiobarbituric acid as studied in the solid, in polar solutions, and on gold nanoparticles. *J. Phys. Chem. C*, *111*(8), 3369-3383. https://doi.org/10.1021/jp0628176

[17] Moskalenko, I.V., Shilovskikh, V.V., Nesterov, P.V., Novikov, A.S., Omarova, M., Sadovnichii, R.V., Gurzhiy, V.V., Orekhov, N.D., & Skorb, E.V. (2023). Supramolecular assemblies of melamine-2-thiobarbiturate and melamine-barbiturate-2-thiobarbiturate: experimental and theoretical studies. *Crystals*, *13*(9), 1302. https://doi.org/10.3390/cryst13091302

[18] Schade, A., Tchernook, I., Bauer, M., Oehlke, A., Breugst, M., Friedrich, J., & Spange, S. (2017). Kinetics of electrophilic alkylations of barbiturate and thiobarbiturate anions. *The Journal of Organic Chemistry, 82*(16), 8476-8488. https://doi.org/10.1021/acs.joc.7b01223

[19] Sharma, A., Zamisa, S.J., Noki, S., Almarhoon, Z., El-Faham, A., la Torre, B.G.d., & Albericio, F. (2018). Crystal structure, spectroscopic studies and theoretical studies of thiobarbituric acid derivatives: Understanding the

hydrogen-bonding patterns. *Acta Crystallogr. Sect. C Struct. Chem.*, *74*, 1703-1714. https://doi.org/10.1107/S2053229618015516

[20] Stewart, J.J.P. (1989). Optimization of parameters for semi-empirical methods I. *J. Comput. Chem.*, *10*, 209-220. https://doi.org/10.1002/jcc.540100208

[21] Stewart, J.J.P. (1989). Optimization of parameters for semi-empirical methods II. *J. Comput. Chem., 10*, 221-264. https://doi.org/10.1002/jcc.540100209

[22] Leach, A.R. (1997). *Molecular modeling*. Essex: Longman.

[23] Kohn, W., & Sham, L.J. (1965). Self-consistent equations including exchange and correlation effects. *Phys. Rev.*, *140*, 1133-1138. https://doi.org/10.1103/PhysRev.140.A1133

[24] Parr, R.G., & Yang, W. (1989). *Density functional theory of atoms and molecules*. London: Oxford University Press.

[25] Becke, A.D. (1988). Density-functional exchange-energy approximation with correct asymptotic behavior. *Phys. Rev. A*, *38*, 3098-3100. https://doi.org/10.1103/PhysRevA.38.3098

[26] Vosko, S.H., Wilk, L., & Nusair, M. (1980). Accurate spin-dependent electron liquid correlation energies for local spin density calculations: a critical analysis. *Can. J. Phys*., *58*, 1200-1211. https://doi.org/10.1139/p80-159

[27] Lee, C., Yang, W., & Parr, R.G. (1988). Development of the Colle-Salvetti correlation energy formula into a functional of the electron density. *Phys. Rev. B*, *37*, 785-789. https://doi.org/10.1103/PhysRevB.37.785

[28] SPARTAN 06 (2006). Wavefunction Inc. Irvine CA, USA.

[29] Richmond, T.J. (1984). Solvent accessible surface area and excluded volume in proteins: Analytical equations for overlapping spheres and implications for the hydrophobic effect. *Journal of Molecular Biology*, *178*(1), 63-89. https://doi.org/10.1016/0022-2836(84)90231-6

[30] Fleming, I. (1976). *Frontier orbitals and organic reactions*. London: Wiley.

[31] Anslyn, E.V., & Dougherty, D.A. (2006). *Modern physical organic chemistry*. Sausalito, California: University Science Books.